

Supporting Information

Structural conversion of three Copper(II) complexes with snapshot observation based on the different crystal colours and morphology

Hao Su^a, Zhongkui Li,^a Junrui Tan,^a Hongwei Ma,^b Li Yan^b and Hui Li^{*a}

*^a Key Laboratory of Cluster Science of Ministry of Education, School of Chemistry and Chemical
Engineering, Beijing Institute of Technology, Beijing 100081, P. R. China*

**E-mail: lihui@bit.edu.cn*

^b Analytical and Testing Center, Beijing Institute of Technology, Beijing 102488, China

Table of Content

S1. Characterization of L, 1, 2 and 3.

Fig. S1. ^1H NMR spectra of L.

Fig. S2. IR spectra of L, 1, 2 and 3.

Fig. S3. Coordination modes of the metal in the compounds 1(a), 2(b) and 3(c).

Fig. S4. Simulation and experiment PXRD pattern of 1, 2 and 3.

Fig. S5. TG curves of 1, 2 and 3.

S2. Crystal Structure Information List of 1, 2 and 3.

Table S1. Selected bond distances (\AA) and angles ($^\circ$) for 1.

Table S2. Selected bond distances (\AA) and angles ($^\circ$) for 2.

Table S3. Selected bond distances (\AA) and angles ($^\circ$) for 3.

S3. Crystal Structure and conversion of 2.

Fig. S6. 2D layer structure of 2.

Fig. S7. The rhombus-shaped crystals of 2 convert quickly to rod-shaped crystals of 1 in methanol solution within 10 min.

Fig. S8. PXRD pattern of 2 after soaking in MeOH solution.

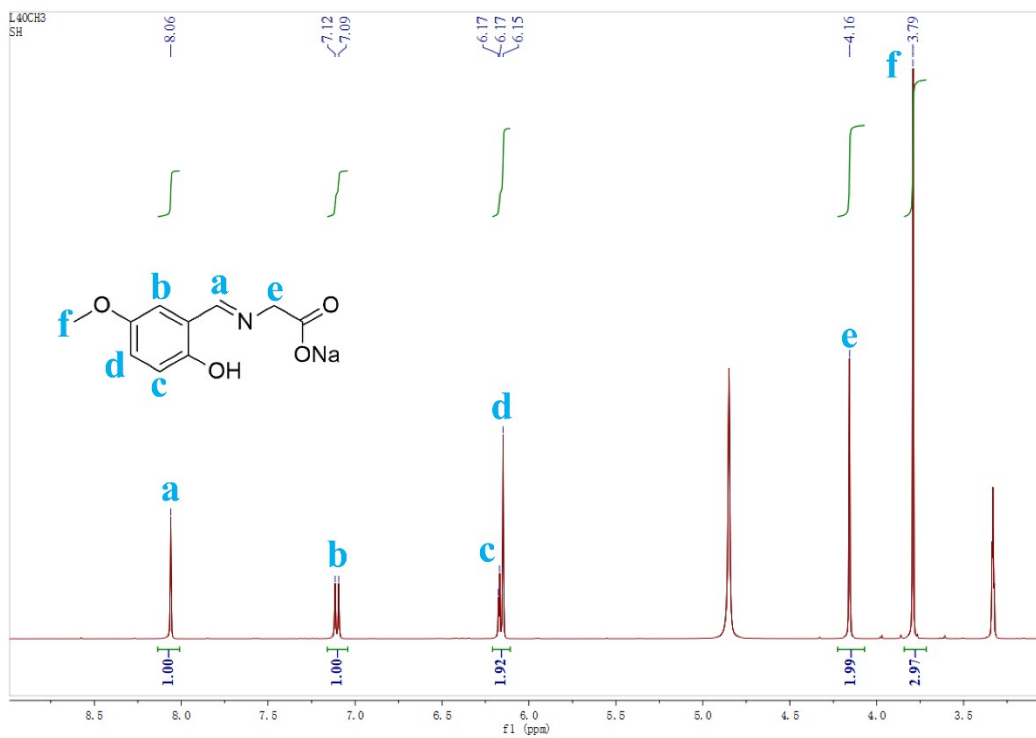


Fig. S1. ^1H NMR spectra of L.

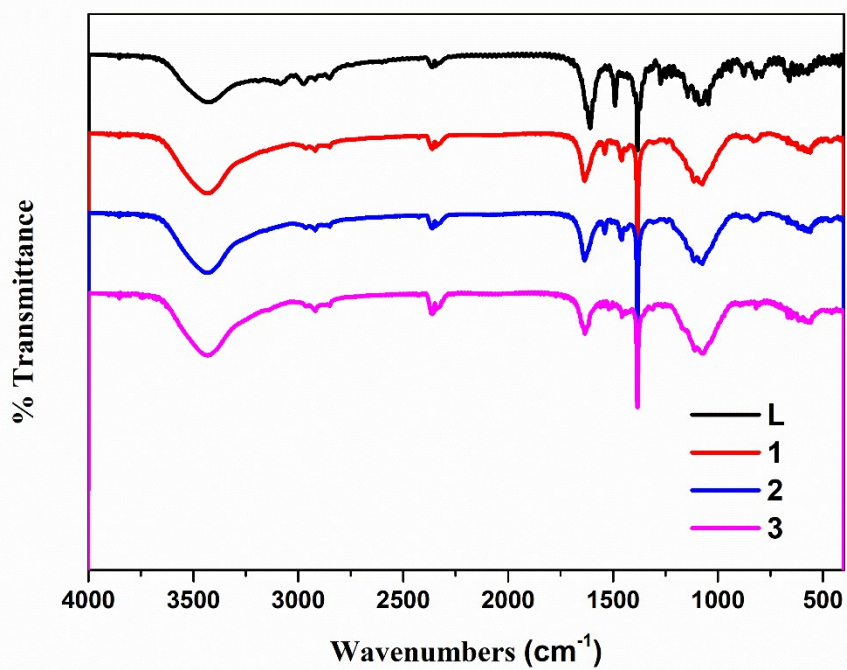


Fig. S2. IR spectra of L, 1, 2 and 3.

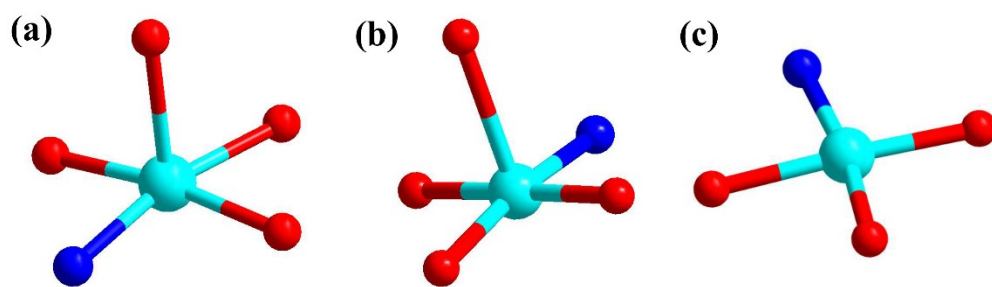


Fig. S3. Coordination modes of the metal in the compounds **1(a)**, **2(b)** and **3(c)**.

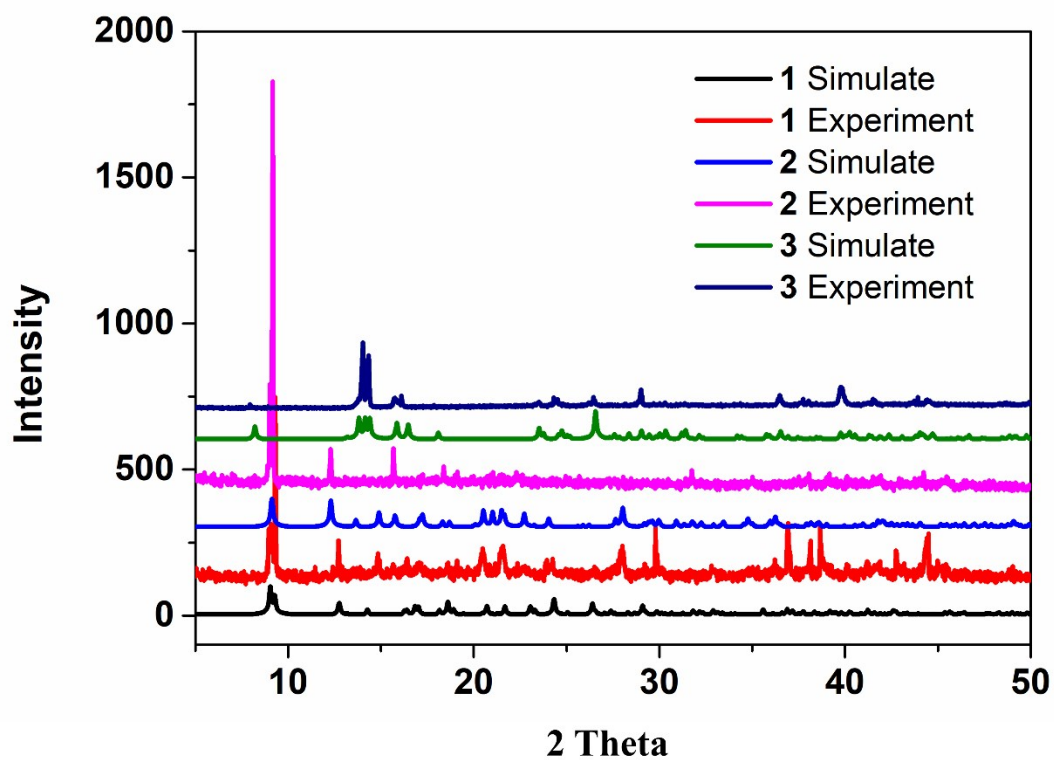


Fig. S4. Simulation and experiment PXR D pattern of 1, 2 and 3.

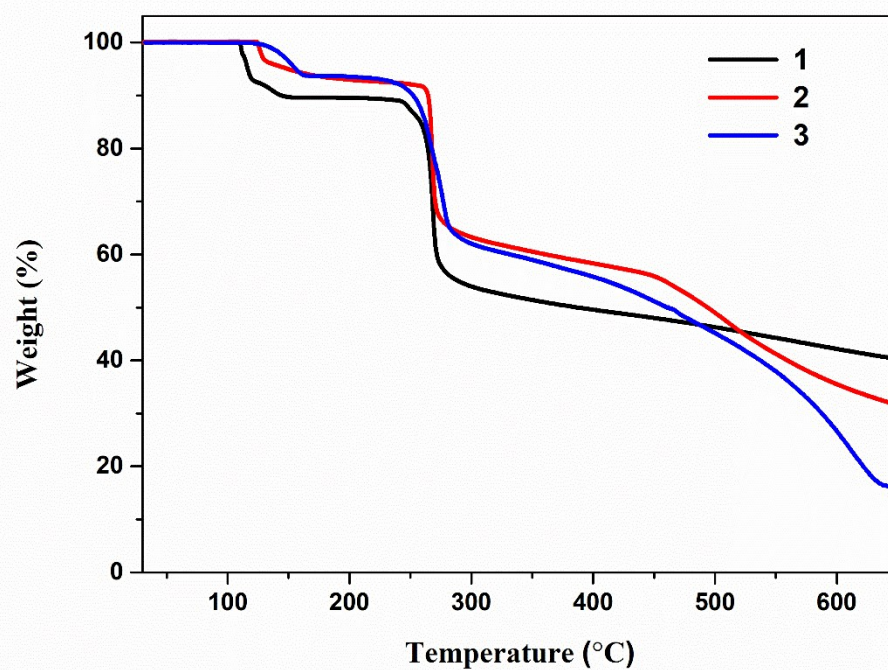


Fig. S5. TG curves of 1, 2 and 3.

Table S1. Selected bond distances (Å) and angles (°) for **1**.

Cu(1)–N(2)	1.929(2)	Cu(1)–O(2)	1.958(2)
Cu(1)–O(1)	1.9659(18)	Cu(1)–O(1)	1.9983(18)
Cu(1)–O(5)	2.252(2)		
N(2)–Cu(1)–O(2)	82.94(9)	N(2)–Cu(1)–O(1)	93.11(8)
O(2)–Cu(1)–O(1)	171.02(8)	N(2)–Cu(1)–O(1)	167.65(9)
O(2)–Cu(1)–O(1)	103.59(8)	O(1)–Cu(1)–O(1)	78.88(8)
N(2)–Cu(1)–O(5)	100.02(9)	O(2)–Cu(1)–O(5)	93.53(9)
O(1)–Cu(1)–O(5)	95.10(8)	O(1)–Cu(1)–O(5)	90.13(8)

Table S2. Selected bond distances (Å) and angles (°) for **2**.

Cu(1)–O(3)	1.906(6)	Cu(1)–N(1)	1.920(8)
Cu(1)–O(2)	1.959(6)	Cu(1)–O(1)	1.962(6)
Cu(1)–O(3)	2.433(6)		
O(3)–Cu(1)–N(1)	94.9(3)	O(3)–Cu(1)–O(2)	85.2(3)
N(1)–Cu(1)–O(2)	171.2(3)	O(3)–Cu(1)–O(1)	177.5(3)
N(1)–Cu(1)–O(1)	83.7(3)	O(2)–Cu(1)–O(1)	95.8(3)
O(3)–Cu(1)–O(3)	90.1(2)	N(1)–Cu(1)–O(3)	95.0(3)
O(2)–Cu(1)–O(3)	93.8(3)	O(1)–Cu(1)–O(3)	92.2(2)

Table S3. Selected bond distances (Å) and angles (°) for **3**.

Cu(1)–O(1)	1.883(2)	Cu(1)–N(1)	1.921(2)
Cu(1)–O(2)	1.931(2)	Cu(1)–O(5)	1.933(2)
O(1)–Cu(1)–N(1)	95.62(9)	O(1)–Cu(1)–O(2)	176.21(10)
N(1)–Cu(1)–O(2)	84.01(10)	O(1)–Cu(1)–O(5)	93.52(10)
N(1)–Cu(1)–O(5)	169.80(10)	O(2)–Cu(1)–O(5)	87.16(10)

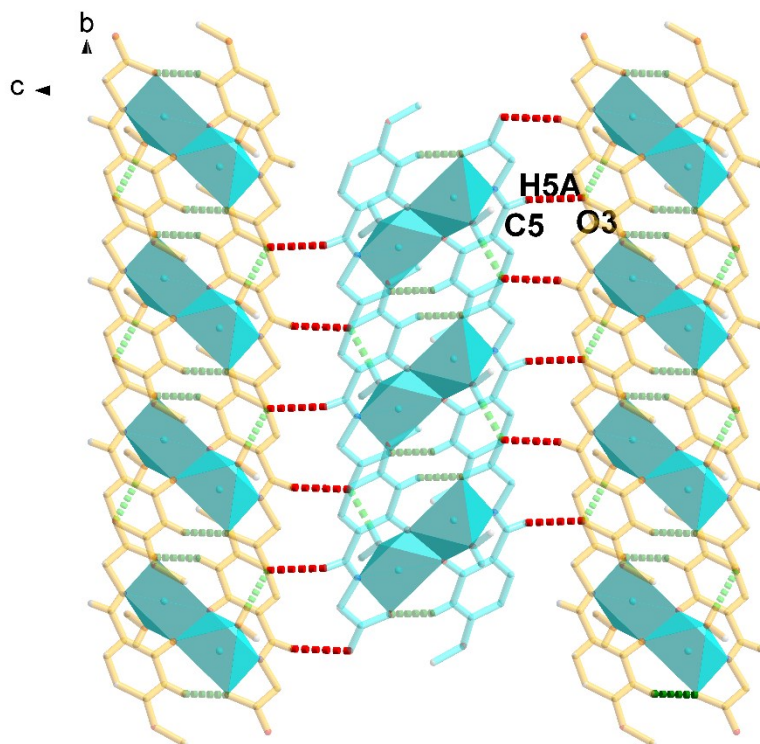


Fig. S6. 2D layer structure of **2**.

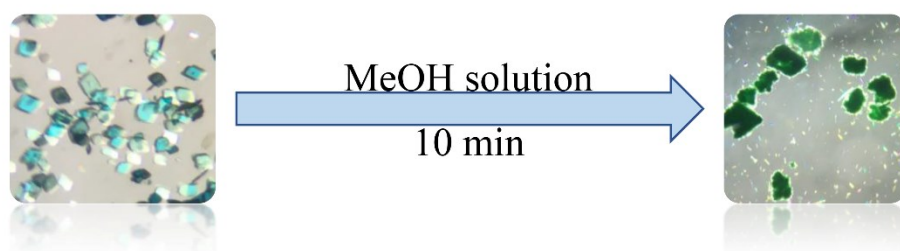


Fig. S7. The rhombus-shaped crystals of **2** convert quickly to rod-shaped crystals of **1** in methanol solution within 10 min.

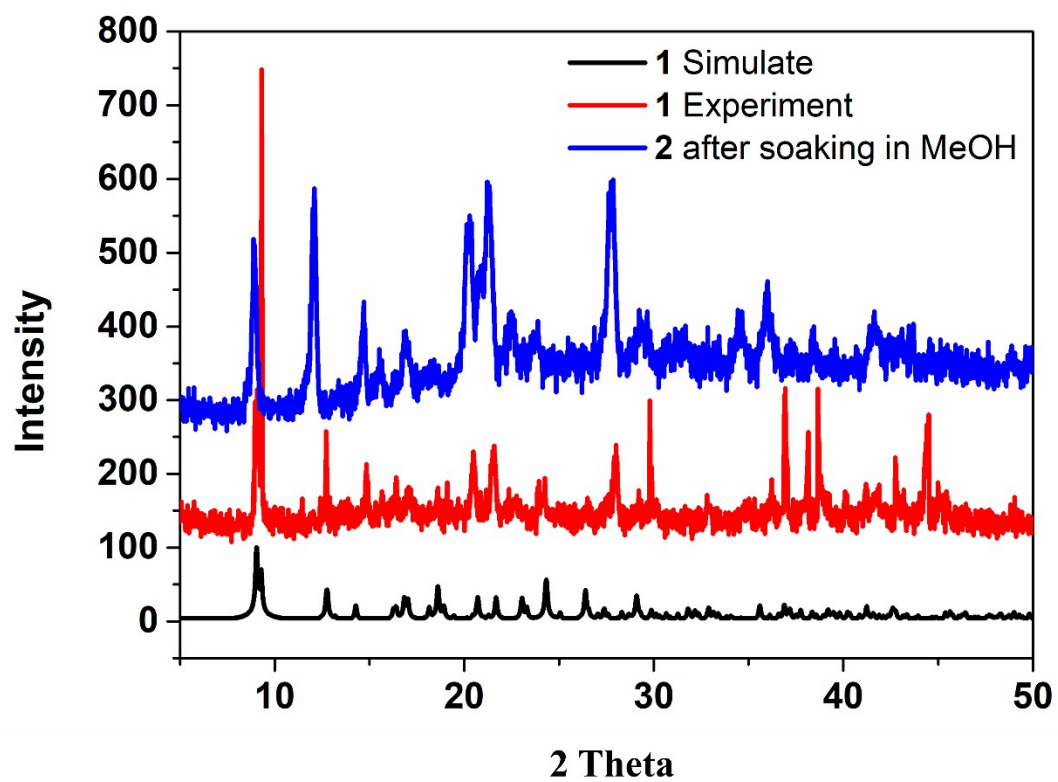


Fig. S8. PXRD pattern of 2 after soaking in MeOH solution.